RESEARCH PAPER

# Evaluation of Anti-Arthritic Activity of Dexamethasone and Curcumin loaded FLPHNPs: A Comparative Preclinical Study Using CFA-Induced Arthritis Model

**Ekta Panchal[1, 2], Shiv Kumar Yadav[2*], Neha Jain[1], Archana Sharma[1*]**

**Affiliation:**

1. Amity Institute of Pharmacy, Amity University Uttar Pradesh, Sector 125, Noida 201303, India
2. Anangpuria School of Pharmaceutical Sciences , Pt. B. D. Sharma University of Health Sciences, Alampur, Faridabad121004, Haryana, India

**Correspondence:**

Dr. Archana Sharma
Associate Professor
Amity Institute of Pharmacy,
Amity University Uttar Pradesh,
Sector 125, Noida 201313, India
E-mail: asharma22@amity.edu
ORCHID ID: 0000-0002-9060-6924

**Abstract**

**Background:** Rheumatoid Arthritis (RA) is a type of incapacitating autoimmune impairment condition which is mainly characterized by long term inflammation of synovium and gradual deterioration of joints. Despite the availability of various effective first-line therapies such as Dexamethasone (Dexa), their non-specificity onto the target site and associated long-term adverse effects restrict broader clinical use. Curcumin (Cur) is a safer alternative that provides anti-inflammatory effect, but has low bioavailability. In this study, the therapeutic effectiveness of Dexa and Cur Loaded Folate-Targeted Lipid Polymer Hybrid Nanoparticles (FLPHNPs) on a Complete Freund's Adjuvant (CFA) induced arthritis in Albino Wistar rats was explored.

**Methodology:** FLPHNPs were synthesized using ionic gelation method and evaluated for various parameters such as particle size, entrapment efficiency, and drug contents. Preclinical studies were conducted using CFA Induced Arthritis Albino Wistar Rats model that were further divided into six groups: control, negative control, Dexa, Cur, Dexa+Cur, and FLPHNPs. Anti-arthritic effectiveness was tested by measuring paw swelling, liver enzymes (SGOT/SGPT), and drug content in plasma and liver tissues.

**Results:** FLPHNPs exhibited the most effective reduction of paw inflammation, getting close to normal size (6.68 mm vs. 6.15 mm in control group). Biochemical indicators of liver functioning (SGOT and SGPT) stayed within physiological range, proving the safety of drug. The content of Dexa and Cur in the plasma and liver was significantly higher in the FLPHNP group, determined by the use of RP-HPLC.

**Conclusion:** FLPHNPs proved their superiority in anti-inflammatory activity and safety compared to conventional drug forms. These results prove the perspective of FLPHNPs as nanotherapy for RA.

**Keywords:** Rheumatoid Arthritis, Curcumin, Dexamethasone, Nanoparticles, Bioavailability, FLPHNPs, CFA model

**How to cite this article:** Ekta Panchal, Shiv Kumar Yadav, Neha Jain, Archana Sharma. Evaluation of Anti-Arthritic Activity of Dexamethasone and Curcumin loaded FLPHNPs: A Comparative Preclinical Study Using CFA-Induced Arthritis Model. Int J Drug Deliv Technol. 2026;16(7):446-455. DOI: 10.25258/ijddt.16.7.48

## .Introduction

Rheumatoid arthritis (RA) is a group of chronic and systemic autoimmune conditions characterized by chronic synovitis, swelling, pain, and degeneration of the joints due to cartilage and bone damage. The multiple causes include immune disorders, inflammatory cytokine production (TNF-α, IL-1β), oxidation, and angiogenesis in the synovial tissue [1,2]. The conventional treatments of RA such as Dexamethasone (Dexa) are effective in reducing inflammation but carry some severe side effects including immunosuppression, liver malfunctioning, and hormonal imbalance [3]. Curcumin (Cur), a powerful anti-inflammatory, antioxidant, and immunomodulatory polyphenolic component of Curcuma longa (turmeric), is currently receiving scientific interest due to its beneficial properties in treating rheumatoid arthritis. Unfortunately, the clinical use of Cur is hindered by the following limitations: low solubility in water, fast metabolic clearance, and poor oral bioavailability. In order to solve the pharmacokinetics problems of Cur, different types of nanoparticles were applied for drug delivery purposes in order to increase its solubility, protect bioactive compounds from metabolism, and sustain its release [4,5].

In this regard, we have earlier described the synthesis and characterization of Folate-Targeted Lipid Polymer Hybrid Nanoparticles (FLPHNPs), which were designed as an innovative carrier system for co-encapsulation of Cur and Dexa. The

FLPHNPs make use of the biocompatibility of lipid polymers, the mucoadhesive and targeted effects of folate-chitosan, and anti-inflammatory synergy of the drugs. Folate modification can additionally improve the tissue targeting because of the upregulation of folate receptors in the inflammatory tissues [3,5].

In the present work, the anti-arthritic effect of FLPHNPs in CFA-induced rat model of arthritis was examined. For comparison, the same tests were performed using free Cur, Dexa, and their combination. The therapeutic results were analyzed in terms of paw edema, parameters of liver enzymes (SGOT/AST and SGPT/ALT), plasma and tissue drug levels, and properties of nanoparticles.

**Materials and Methods**

Dexamethasone and curcumin with 98% purity level were procured from GLR Innovations, New Delhi, India. Other chemicals and reagents details used in formulation were described in previous research work. Complete Freund's adjuvant (CFA), sterile mineral oil, ether, L-aspartate, α-ketoglutarate, NADH (β-nicotinamide adenine dinucleotide reduced), MDH (malate dehydrogenase), DNPH (2,4-dinitrophenylhydrazine) and diethyl ether were purchased from Sigma-Aldrich (St. Louis, MO, USA). NaOH and analytical-grade methanol were obtained from commercial sources. Ultra-pure water was used for all aqueous reagent preparations. All chemicals were of analytical grade and used strictly in accordance with the suppliers' guidelines.

**Preparation of FLPHNPs loaded with Dexa and Cur**

The formulation of FLPHNPs was carried out according to the optimized protocol previously reported by our research group. Since the formulation methodology has already been published, only a brief description is presented here. The detailed preparation procedure, optimization, and characterization are available in Panchal et al. (2025) [6,7]. Initially, Folic Acid (FA) was conjugated to chitosan (Chi) via a carbodiimide coupling reaction using N-Hydroxysuccinimide (NHS), N, N′-dicyclohexylcarbodiimide (DCC), and triethylamine in dimethyl sulfoxide (DMSO) under dark conditions, followed by filtration, washing, and lyophilisation [8,9]. The NHS-activated FA was then reacted with Chi in acetate buffer (pH 5.6), maintaining pH 9.0, and then FA-Chi conjugates were purified by centrifugation and washing techniques. Drug loaded FLPHNPs (i.e. Dexa and Cur (1:1 molar ratio) were formulated by ionic gelation between cationic chitosan and anionic soya lecithin, involving drop-wise addition of the ethanolic lipid phase into the aqueous polymer phase under high-speed stirring and homogenization [8,10].

**Entrapment Efficiency and Particle Size Analysis**

Entrapment efficiency for Cur and Dexa was evaluated by centrifuging the nanoparticle dispersion and measuring free drug in the supernatant using UV-Vis spectroscopy at appropriate wavelengths (λmax: 242 nm for Dexa, 425 nm for Cur). Particle size was measured using dynamic light scattering (DLS) (Malvern Zetasizer Nano ZS) [11,12,13].

**Animal selection and procurement**

Healthy Wistar rats (200-250g) were procured from Deshpande Laboratories Pvt. Ltd., Bhopal, India. The animals housing conditions were regulated properly for stable temperature and humidity which were followed through the standard diet and water. The animal used in the study was approved by the IAEC, which is certified by the committee for CPCSEA, in India, under approval no. - CPCSEA/IAEC03202463.

**CFA-Induced Arthritis Model**

Rats were randomly divided into six groups (n=6) and arthritis was induced using a single sub-plantar injection of CFA (0.1 ml) into the left hind paw. Drug treatments (FLPHNPs, Dexa, Cur, and Dexa+Cur) were administered daily for 21 days post-induction. Paw dimensions were measured using a vernier caliper to evaluate inflammation [14,15].

**Biochemical Analysis (Liver Enzymes)**

Blood was collected via retro-orbital plexus and serum was separated. Serum Glutamic Oxaloacetic Transaminase (SGOT) also refer as {Aspartate Aminotransferase (AST)} and Serum Glutamic Pyruvic Transaminase (SGPT) also refer as {Alanine Aminotransferase (ALT)} levels were analyzed using standard colorimetric methods as per the IFCC recommendations:

**SGOT**: SGOT (AST) is a type of enzyme that plays a crucial role in amino acid metabolism and energy production (exclusively in the malate-aspartate shuttle). Its level was measured via DNPH-pyruvate reaction at 505 nm after incubation. SGOT (AST) activity was evaluated according to standard of the International Federation of Clinical Chemistry (IFCC) utilizing the UV kinetic approach.

In this reaction, SGOT (AST) catalyzes transamination of L-aspartate and α-ketoglutarate and gives rise to oxaloacetate and L-glutamate. Later on, with the presence of MDH (malate dehydrogenase) and NADH, oxaloacetate gets converted into malate. The rate of conversion of NADH to $NAD^+$ is determined from the decline in absorbance at 340 nm that measures the AST enzyme activity. The rate of oxidation of NADH to $NAD^+$ is determined from the decrease in

absorbance at 340 nm that is directly proportional to AST activity. In other words, 1.0 mL of enzyme reagent (L-aspartate, α-ketoglutarate, NADH, and MDH) was mixed with 0.1 mL of serum. The absorbance was measured at 340 nm at every 30 seconds for 2-3 minutes at 25-30°C [18,19].

**SGPT**: SGPT (ALT) is a type of enzyme which is primarily found inside liver cells (hepatocytes). Its level was measured using NADH oxidation method at 340 nm at 25–30°C (kit-based method, modified). SGPT (ALT) activity was estimated using the Reitman and Frankel colorimetric method. The assay procedure relies onto the transamination of L-alanine and α-ketoglutarate to pyruvate and glutamate by using serum ALT as a result of which the synthesized pyruvate formed further reacts with 2, 4-dinitrophenylhydrazine (DNPH) to form a brown-colored hydrazone product. Briefly, 0.5 mL of substrate reagent was initially pre-incubated at 37°C for about 3 minutes which was then followed by the combining with 0.1 mL serum. After 30 minutes of incubation period at 37°C, 0.5 mL DNPH was introduced and allowed it to stand for 20 minutes at room temperature. Thereafter, 5 mL of NaOH was mixed with the above solution, and then the optical density was measured at 505 nm. ALT activity was calculated by comparing the absorbance with that of a pyruvate standard and expressed in IU/L [16,17].

**Tissue Drug Distribution**

The animals were sacrificed 10 hours post final dosage under anesthesia. Hepatic tissue samples were obtained, washed with ice cold normal saline to wash off blood contamination, dried and then weighed. Each sample (0.5 g) was homogenized in 4 mL phosphate-buffered saline (PBS, pH 7.4) using a tissue homogenizer on ice. The homogenate was centrifuged at 10,000 rpm for 15 minutes at 4°C [20,21]. The clear supernatant was mixed with an equal volume of cold methanol to precipitate proteins and centrifuged again. The resulting supernatant was filtered using a 0.22 µm syringe filter and analyzed by RP-HPLC under the following conditions: BDS Hypersil C8 column, mobile phase of acetonitrile:water (60:40, pH adjusted to ~3.0 with orthophosphoric acid), flow rate 1.0 mL/min, UV detection at 242 nm. Quantification was performed by comparison with standard calibration curves prepared in liver homogenate matrix [22,23].

**Plasma Drug Estimation by HPLC**

Blood samples were collected at 0, 1, 5, 10, and 15 hours post-dose. Plasma was separated and proteins were precipitated with methanol (1:1). After centrifugation, the supernatant was injected into HPLC. Plasma concentrations of Cur and Dexa were quantified using a validated reverse-phase high-performance liquid chromatography (RP-HPLC) method. Blood samples were collected at predetermined intervals (0, 1, 5, 10, and 15 hours) via retro-orbital puncture and centrifuged to separate plasma [24, 25]. Proteins were precipitated by mixing plasma with methanol (1:1 v/v), followed by centrifugation at 10,000 rpm for 10 minutes. The supernatant was filtered and injected into the HPLC system equipped with a BDS Hypersil C8 column. The mobile phase consisted of acetonitrile and water (adjusted to appropriate pH with acid) in isocratic mode at a flow rate of 1.0 mL/min. Detection was performed using a UV detector at 242 nm. Drug concentrations were determined by comparing peak areas with standard calibration curves of known concentrations [26,27]. The method parameters were:

- Column: BDS Hypersil C8
- Flow rate: 1.0 mL/min
- Detection: 242 nm
- Mobile phase: Acetonitrile:Water (with acidification)

**Statistical Analysis**

Data were expressed as mean ± SD. Statistical differences between groups were analyzed using one-way ANOVA followed by Tukey's post hoc test. A p-value < 0.05 was considered significant [28].

**Results**

**Characterisation of optimized FLPHNPs formulation**

The optimized FLPHNPs formulation (D18) composed of 88.27 mg folate-chitosan and 50 mg phospholipid (soya lecithin), and an equal amount (50 mg each) of Dexa and Cur which was further processed at a homogenization speed of 10,587.99 rpm, demonstrated high drug encapsulation and favourable particle size.

This composition has been chosen to ensure efficient co-encapsulation and synergistic medicinal action. In our study the entrapment efficiencies have been found to be 89.12% for Dexa and 98.27% for Cur which is in line with our theoretical calculations. The size of particles has been measured to be 287.88 ± 0.83 nm suggesting a nano-scale formulation for drug delivery (Table 1). The results of the other methods of characterizations were also carried out and they have been presented in an earlier work.

**Table 1:** Formulation parameters and characterization of FLPHNPs Formulation (D18)

| Formulation code | Amount of Dru | Amount of Dru | Folate Chito | Phospholipid (Soy | Homogenization speed | Predicted values | | | Experimental Values | | |
|---|---|---|---|---|---|---|---|---|---|---|---|
| | | | | | | % Entrapm | % entrapm | Particle | % entrapm | % entrapm | Particle |

| e | g (Dexa) (mg) | g (Cur) (mg) | san (mg) | alecithin) (mg) | | entofDexa | entofCur | size (nm) | entofDexa | entofCur | size (nm) |
|---|---|---|---|---|---|---|---|---|---|---|---|
| D18 | 50 | 50 | 88.27 | 50 | 10587.99 | 90.453386 | 97.844498 | 286.552 | 89.1191±0.0870 | 98.2721±0.1110 | 287.88±0.831 |

**Evaluation of Paw Dimension – Inflammation Assessment**

Paw edema is a quantitative indicator of the severity of the inflammation present in an arthritic animal model. In this experiment, inflammation was induced by using Complete Freund's Adjuvant (CFA), and paw thickness was measured by using vernier caliper.

Untreated arthritic mice (Negative control) showed a significant increase in paw size (9.73±0.14 mm) as compared to untreated uninduced (Control) (6.15±0.05 mm) demonstrating successful induction of animal model (Figure 1 and 2). Treatment with FLPHNPs showed the most significant decrease in swelling of paws (6.68±0.12 mm) and almost returned them to physiological normal size. The next one in line was the Dexa + Cur group (7.35±0.14 mm), followed by the Dexa treatment alone (7.72±0.15 mm) and Cur treatment alone (8.55±0.14 mm). Hence, the co-delivery system of nanoparticles exhibited better anti-inflammatory activity (Table 2).

**Table 2:** Effect of various treatments on paw dimensions in CFA-induced arthritic rats

| Group | Avg. Normal Paw(mm) | Avg. Inflamed Paw(mm) |
|---|---|---|
| Uninduced | | |
| Untreated | 6.15±0.05 | 9.73±0.14 |
| Dexa | 6.15±0.05 | 7.72±0.15 |
| Cur | 6.17±0.05 | 8.55±0.14 |
| Dexa + Cur | 6.17±0.05 | 7.35±0.14 |
| FLPHNPs | 6.13±0.05 | 6.68±0.12 |

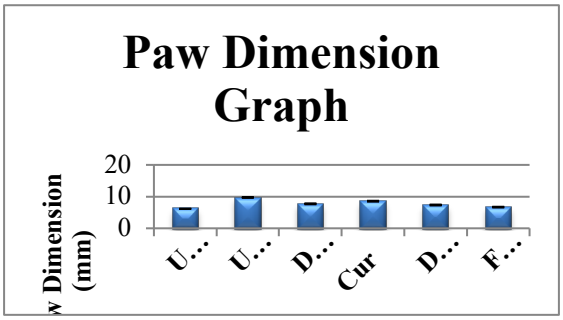


**Figure 1:** Treatment effects on paw edema: Treatment with FLPHNPs showed maximum anti-inflammatory activity, which indicated maximal efficacy in reducing paw thickness back to physiological normal value. The order of effectiveness was FLPHNPs > Dexa + Cur > Dexa ~ Cur.

**Figure 2:** Effects of FLPHNPs and other interventions on paw thickness in arthritis-induced CFA rats. This figure describes the comparison between paw sizes (mm) in different experimental groups. There was increased paw swelling in the induced untreated group whereas paw thickness decreased significantly with FLPHNPs, approaching normal levels. Results are presented in mean values of paw thickness for each group.

**SGOT (AST) Levels (IU/L) – Liver Function**

Elevated serum transaminases, especially SGOT (AST), are sensitive clinical markers of cell membrane permeabilization, tissue strain or hepatocellular necrosis. Under physiologic conditions, SGOT is largely contained within the cellular cytoplasm and mitochondria, but is released into the systemic circulation following cellular disruption. The catalytic concentration of SGOT (AST) was calculated by tracking the spectrophotometric decrease of NADH at 340 nm. In this two-step reaction, AST-driven conversion of L-aspartate yields oxaloacetate, which is rapidly consumed by malate dehydrogenase alongside NADH oxidation. The observed rate of absorbance loss at 340 nm served as a direct quantitative measure of enzymatic activity. Briefly, 1 mL of enzyme reagent was mixed with 5 mL of start reagent to prepare the working reagent. Subsequently, 100 µL of the working reagent was mixed with 20 µL of the serum sample. The absorbance was analysed at 340 nm at 25–30 °C at

2 and 3 minutes. The variation in the absorbance level (ΔA/min) was calculated and multiplied by a factor of 952 to find out the SGOT enzyme activity, which was expressed as IU/L (Table 3).

Reagents volumes were scaled down in proportion as required. All interventions resulted in normal or reduced SGOT levels, demonstrating absence of liver toxicity. FLPHNPs retained liver function as healthy controls (figure 3).

In the present study, serum SGOT activity was elevated in the untreated group after the induction of disease suggesting active cellular stress. The treatment with FLPHNPs resulted in a significant therapeutic response with serum SGOT levels (approx 109.47 IU/L) coming back to basal levels similar to the normal uninduced control group (approx 109.5 IU/L).The recovery effect was comparable with the standard drug treatment (Dexa) and better than free curcumin (Cur), suggesting that the FLPHNP formulation increases the drug stability, cellular uptake and bioactivity. FLPHNPs are able to maintain the structural integrity of the cells by reducing the membrane permeability and preventing the leakage of the enzymes to the vascular bed. The synthesized FLPHNPs maintained liver function similar to controls (Figure 3).

**Table 3:** Serum SGOT (AST) levels in different treatment groups

| Group | Average SGOT (IU/L) |
|---|---|
| Uninduced Untreated | 109.5±4.36 |
| Induced Untreated | 112.38±4.63 |
| Dexa | 109.47±5.9 |
| Cur | 110.62±4.97 |
| Dexa + Cur | 111.27±6.31 |
| FLPHNPs | 109.4±4.36 |

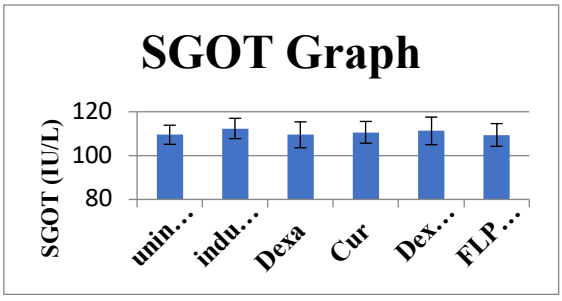


**Figure 3:** Average serum SGOT (AST) level following interventions in arthritis-induced CFA rats. This figure shows the average serum SGOT levels (IU/L) of all experimental groups. There was a slight increase in the AST level of the induced untreated group compared to the control. The FLPHNPs treated animals had a level close to the basal one, thus showing that there was no hepatotoxic effect and hence good biocompatibility of the formulation.

**SGPT (ALT) Levels (IU/L) – Liver Function**

Serum alanine aminotransferase (SGPT/ALT) is a cytosolic enzyme mainly located in the hepatocytes and is therefore a very specific marker for liver cell membrane instability, inflammation and cellular injury. When the membrane is damaged or necrosis begins, intracellular SGPT leaks out rapidly into the systemic circulation, and the enzymatic activity of serum increases.

SGPT (ALT) mediates the transamination of an amino group from L-alanine to α- ketoglutarate, thus generating pyruvate and glutamate. The generated pyruvate forms hydrazone complex with 2, 4- dinitrophenylhydrazine (DNPH), which is quantified using spectrophotometry. In summary, 0.3 mL of substrate solution, 0.2 mL of pyruvate standard, 0.1 mL of distilled water (DW), and 0.05 mL of DNPH solution were taken and kept at RT for 20 minutes.

The absorbance was measured and used to calibrate the assay. For sample analysis, 0.50 mL of substrate reagent was pre-incubated at 37 °C for 3 min. Subsequently, 0.1 mL of serum sample was introduced, mix thoroughly, and incubated at 37 °C for 30 min. After completion of incubation period, 0.5 mL of DNPH reagent was added, mixed, and allowed to stand at RT for approx 20 min. Finally, 5 mL of NaOH reagent was mixed, thoroughly homogenized, and allowed to stand for 10 min at RT before measuring the absorbance at 505 nm. Reagents volumes were scaled down in proportion as required.

In this study, untreated induced group showed increased SGPT levels in comparison to treated groups. FLPHNPs administration successfully suppressed serum SGPT levels (approx 121.93 IU/L) reducing the enzyme release below the induced untreated control (126.87 IU/L) and also the healthy uninduced baseline (approx 126.3 IU/L).

FLPHNPs mediated enzymatic reduction was comparable to the free Cur and better than the standard Dexamethasone (Dex) monotherapy. The reduction by FLPHNPs of the circulating SGPT is indicative of the possibility of the formulation to stabilize hepatocyte membranes, scavenge reactive

radical species and limit leakage of enzymatic factors. The nanoencapsulated delivery system is likely to promote sustained active transport and increased intracellular accumulation thereby more effectively relieve cellular stress caused by disease than traditional therapeutic methods. Likewise, FLPHNPs and Cur displayed enhanced liver enzyme activities, indicating that they possess hepatoprotective, anti-inflammatory and safe properties, as depicted in Fig. 4 (Table 4).

**Table 4:** Serum SGPT (ALT) Level in different treatment groups

| Group | Average SGPT IU/L |
|---|---|
| Uninduced Untreated | 126.38±1.49 |
| Induced Untreated | 126.87±1.43 |
| Dexa | 123.60±5.45 |
| Cur | 120.85±5.31 |
| Dexa + Cur | 124.58±4.46 |
| FLPHNPs | 121.93±5.4 |

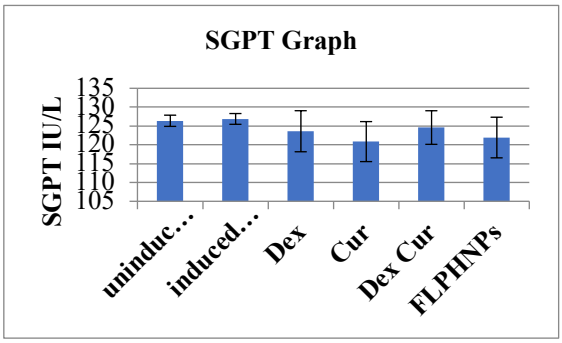


**Figure 4: Serum SGPT (ALT) concentration in different experimental groups:** It depicts SGPT enzyme activity (IU/L) as an indicator of liver functionality. The highest serum SGPT concentration was recorded in the induced group without any medication, and treatments with FLPHNPs and Cur resulted in decreased SGPT concentration, showing its protective action on the liver and higher tolerance of treatments.

**Tissue Drug Distribution (10h post-dose)**

At 10 h post-administration, tissue distribution was different between various formulations. FLPHNP/C and FLPHNP/D had significantly higher amounts of tissue concentration, which were found to be 0.105±0.0022µg/mL and 0.128±0.0051µg/mL, respectively. In comparison to each other, FLPHNP/D had higher tissue uptake than FLPHNP/C, indicating that the former formulation showed higher tissue uptake/clearance. In comparison to free drugs, tissue concentration was much lower, 0.014 ± 0.0012µg/mL and 0.013±0.0032µg/mL for Dexa and Cur, respectively. It is evident from the data obtained that nanoparticle formulations have approximately 7-10 times more tissue concentration than free compounds which suggest that the nano-encapsulation process is very effective in increasing the bioavailability of the drugs in target tissues.

These results suggest that FLPHNP-based delivery system is effective to increase drug distribution and retention in target tissues, which is probably due to increased permeability, decreased systemic clearance and potential sustained-release behavior. The slight increase in accumulation with FLPHNP/D compared to FLPHNP/C may be due to formulation-dependent differences in the properties of the particles, such as their size, surface properties, or drug encapsulation efficiency (Figure 5). On the contrary, the decrease in the tissue levels of free Dexa and Cur is rapid, highlighting the limited stability and faster metabolic elimination of free drugs when administered without a delivery system (Table 5). Taken together, the results are consistent with the benefit of nanoparticle-mediated delivery to increase tissue exposure, which may translate into improved therapeutic efficacy and biological longevity.

**Table 5:** Tissue drug distribution in different treatment groups

| Compound | Tissue Concentration (µg/ml) |
|---|---|
| FLPHNP/C | 0.105±0.0022 |
| FLPHNP/D | 0.128±0.0051 |
| Dexa | 0.014±0.0012 |
| Cur | 0.013±0.0032 |

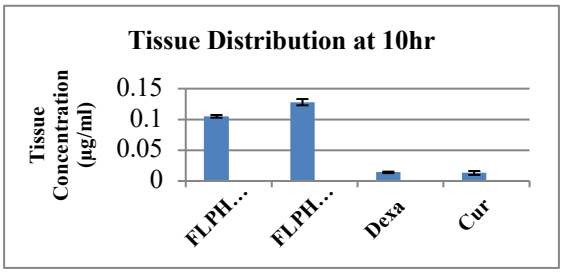


**Figure 5:** Distribution of Dexa and Cur in liver tissue (µg/mL). The figure represents the concentrations of Dexa and Cur in liver at 10 h after administration. The tissue levels of FLPHNPs

were significantly higher than that of free drug formulations indicating improved bioavailability and sustained tissue retention through nanoparticle delivery.

**In vivo pharmacokinetics evaluation**

The plasma drug concentration profile of Dexa and Cur was examined. Drug levels in plasma were determined by RP-HPLC at various time intervals after drug dosing. The plasma drug concentration was higher and more sustained in the FLPHNP-treated group, and peak levels at 5-10 h suggested enhanced absorption and prolonged circulation. FLPHNPs lead to significantly higher tissue concentrations, supporting better bioavailability compared to standard Dexa or Cur as depicted in Figures 6 and 7 (Table 6 and 7).

**Table 6:** Comparative plasma drug concentration profile of Cur delivered via FLPHNPs versus free drug at various time points.

| Time (h) | FLPHNP/C (µg/mL) | Cur (µg/mL) |
|---|---|---|
| 0 | 0 | 0 |
| 1 | 0.02 | 0.098 |
| 4 | 0.07 | 0.06 |
| 7 | 0.095 | 0.03 |
| 10 | 0.092 | 0.01 |
| 15 | 0.014 | 0.005 |

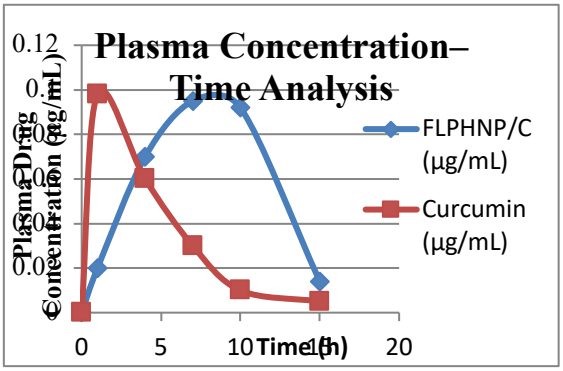


**Figure 6: Plasma concentration vs. time curve.** In vivo pharmacokinetic evaluation showing plasma drug levels (µg/mL) over a 15-hour period for FLPHNP/C and free Curcumin.

**Table 7:** Comparative plasma drug concentration profile of Dexa delivered via FLPHNPs versus free drug at various time points.

| Time (h) | FLPHNP/D (µg/mL) | Dexa (µg/mL) |
|---|---|---|
| 0 | 0 | 0 |
| 1 | 0.025 | 0.115 |
| 4 | 0.125 | 0.08 |
| 7 | 0.15 | 0.045 |
| 10 | 0.14 | 0.02 |
| 15 | 0.015 | 0.005 |

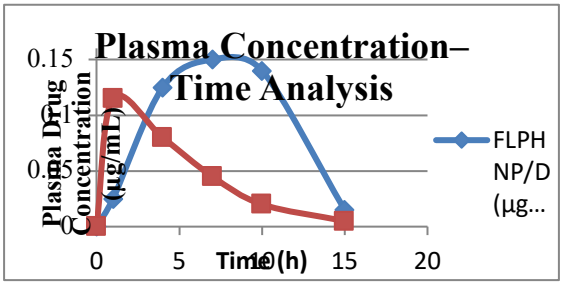


**Figure 7: Plasma concentration vs. time curve.** In vivo pharmacokinetic evaluation showing plasma drug levels (µg/mL) over a 15-hour period for FLPHNP/C and free Dexa.

**HPLC Data (Plasma Levels)**

Blood was withdrawn by orbital puncture 0,1,5,10,15 hrs and plasma was separated by centrifugation. Plasma samples were precipitated by 1:1 methanol. Methanol samples were centrifuged to remove suspended debries. The methanol samples were analyzed with following parameters RP-HPLC on a BDS Hypersil C8 column; mobile phase: as mentioned, flow rate 1.0 mL min-1 and a UV detector at 242nm. Time-dependent plasma concentrations confirm higher peak levels for FLPHNPs, especially at 5 and 10 hrs, validating its sustained release or improved absorption.

**Chromatogram**

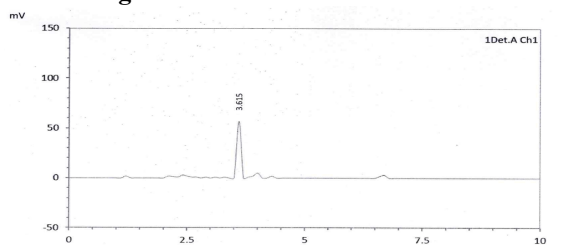


| Peak | Name | Ret. Time | Area |
|---|---|---|---|
| 1. | Dexamethasone | 3.615 | 11476 |

**Figure 8:** HPLC chromatogram of Dexamethasone shows the retention time and peak area of Dexamethasone as detected at 3.615 minutes under

the defined HPLC conditions, confirming its identification and quantification in plasma samples.

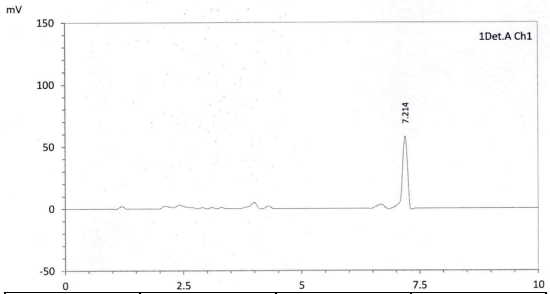


| Peak | Name | Ret. Time | Area |
|---|---|---|---|
| 1. | Curcumin | 7.214 | 12214 |

**Figure 9:** HPLC chromatogram of Curcumin displays the Curcumin peak at 7.214 minutes. The retention time and peak characteristics were consistent with the standard curve, validating the presence of Curcumin in plasma after FLPHNP administration.

**Discussion**

The results of this study demonstrated the potential of Folate-Linked Phospholipid Hybrid Nanoparticles (FLPHNPs) as a novel delivery system for enhancing the therapeutic effects of Dexa and Cur in RA. The pathogenesis of RA is defined by immune-mediated inflammation, oxidative stress and tissue destruction. The CFA-induced arthritis model successfully mimicked these pathological features and served as a reliable preclinical platform to assess anti-arthritic efficacy [29,30]. The nanoparticle formulation (D18) showed an optimum particle size (~287 nm) and high entrapment efficiency for both drugs (Dexa: ~89%, Cur: ~98%,), which is essential for improving the systemic bioavailability. FLPHNPs showed the highest reduction in paw edema compared with free drugs and their combination, almost restoring paw thickness to normal levels. This indicates a synergistic anti-inflammatory effect and improved tissue targeting probably mediated by folate-chitosan conjugation [31].

Biochemical examination also confirmed the safety of the formulation. Notably, free Dexamethasone and Curcumin individually caused modest effects on SGOT and SGPT levels, whereas FLPHNPs kept liver enzyme values close to baseline. This indicates reduced hepatic burden and systemic toxicity, which is particularly relevant in light of potential hepatotoxicity with long-term corticosteroid therapy. Furthermore, pharmacokinetic study using HPLC showed that the FLPHNPs achieved significantly higher levels of both Curcumin and Dexamethasone in plasma and liver tissues, indicating improved absorption and prolonged circulation time. The folate functionalized surface likely triggered increased uptake by tissues, as folate receptors are upregulated in inflamed tissues like arthritic joints and liver [29,32].

These all results taken collectively prove the superiority of FLPHNPs over other therapeutic approaches. With an ability to increase bioavailability while decreasing toxicity, FLPHNPs can be used as a promising dual-drug nanocarrier for the successful treatment of rheumatoid arthritis.

**Conclusion**

The current study has been able to show that Folates Linked Phospholipid Hybrid Nano Particles (FLPHNPs) carrying Dexamethasone and Curcumin can be considered a highly advanced treatment method for rheumatoid arthritis. This is because the nano-particle has been found to have a higher anti-inflammatory activity due to its ability to reduce the paw edema in the arthritis rats induced with CFA. Moreover, FLPHNPs were found to keep the liver enzymes within the acceptable range, thus showing high safety profile. Increased drug concentration in the plasma and liver tissue shows increased bioavailability and sustained release due to targeting through the help of folate nanoparticles. All these results collectively prove the efficiency of using FLPHNPs as a promising drug delivery system for dual therapy of inflammatory diseases such as rheumatoid arthritis, which is more efficient in terms of efficacy and minimal side effects.

**Conflict of interest**

The authors declare no conflict of interest.

**Funding source**

Nil

**Author Contributions**

Ekta Panchal contributed to the design of the study and wrote the first draft. The article was revised and evaluated by Shiv Kumar Yadav. Neha Jain edited the manuscript and helped understand the data. Archana Sharma was involved in the planning, oversight, and editing of the study's manuscript.

**References**

1. Gharat S, Pandya A, Kulkarni D, Momin M. Unravelling the potential of nanocarriers to deliver Curcumin for the management of Rheumatoid Arthritis. Journal of drug delivery science and technology. 2023 Sep 1;87:104742.
2. Syed A, Karwa P, Vemula KD, Salwa. Multifunctional nanoparticles encapsulating methotrexate and curcumin for holistic management of rheumatoid arthritis: In-vitro and pre-clinical assessment. Drug Development and Industrial Pharmacy. 2023 Aug 3;49(8):536-49.
3. Yi Z, Ran Y, Chen X, Tong Q, Ma L, Tan Y, Ma X, Li X. Tea polyphenol carrier-enhanced dexamethasone nanomedicines for inflammation-targeted treatment of rheumatoid

arthritis. Journal of Materials Chemistry B. 2023 Dec 13;11(48):11505-18.
4. Sun J, Du J, Liu X, An J, Hu Y, Wang J, Zhu F, Feng H, Cheng S, Tian H, Mei X. Chondroitin sulfate-modified tragacanth gum–gelatin composite nanocapsules loaded with curcumin nanocrystals for the treatment of arthritis. Journal of Nanobiotechnology. 2024 May 20;22(1):270.
5. Logesh K, Raj B, Bhaskaran M, Thirumaleshwar S, Gangadharappa HV, Osmani RA, Spandana KA. Nanoparticulate drug delivery systems for the treatment of rheumatoid arthritis: a comprehensive review. Journal of Drug Delivery Science and Technology. 2023 Mar 1;81:104241.
6. Panchal E, Yadav SK, Jain N, Chauhan M, Sharma A. Design and optimization of folate-targeted lipid-polymer hybrid nanoparticles co-encapsulating dexamethasone and curcumin for synergistic anti-inflammatory efficacy in rheumatoid arthritis. Journal of Applied Pharmaceutical Research. 2025 Oct 31;13(5):91-113.
7. Ullah S, Azad AK, Nawaz A, Shah KU, Iqbal M, Albadrani GM, Al-Joufi FA, Sayed AA, Abdel-Daim MM. 5-fluorouracil-loaded folic-acid-fabricated chitosan nanoparticles for site-targeted drug delivery cargo. Polymers. 2022 May 13;14(10):2010.
8. Hanan H, Pervaiz F, Ijaz M, Arshad T, Saeed K, Javaid SM, Hussain P, Majeed A. Novel pH-responsive folate conjugated chitosan and thiolated carboxymethyl cellulose based nanoparticles: potential approach for site-specific targeting in colon cancer treatment. International Journal of Biological Macromolecules. 2025 Jun 1;311:143952.
9. Jha R, Mayanovic RA. A review of the preparation, characterization, and applications of chitosan nanoparticles in nanomedicine. Nanomaterials. 2023 Apr 7;13(8):1302.
10. Jain S, Kumar M, Kumar P, Verma J, Rosenholm JM, Bansal KK, Vaidya A. Lipid–polymer hybrid nanosystems: a rational fusion for advanced therapeutic delivery. Journal of Functional Biomaterials. 2023 Aug 23;14(9):437.
11. Patra S, Dey J, Chakraborty A. Physicochemical characterization, stability, and in vitro evaluation of curcumin-loaded solid lipid nanoparticles prepared using biocompatible synthetic lipids. ACS Applied Bio Materials. 2023 Jul 5;6(7):2785-94.
12. Dawud H, Abu Ammar A. Rapidly dissolving microneedles for the delivery of steroid-loaded nanoparticles intended for the treatment of inflammatory skin diseases. Pharmaceutics. 2023 Feb;15(2):526.
13. Sivadasan D, Sultan MH, Madkhali O, Almoshari Y, Thangavel N. Polymeric lipid hybrid nanoparticles (plns) as emerging drug delivery platform—A comprehensive review of their properties, preparation methods, and therapeutic applications. Pharmaceutics. 2021 Aug 18;13(8):1291.
14. Gharat S, Basudkar V, Momin M. In-vitro and in-vivo evaluation of the developed curcumin-cyclosporine-loaded nanoemulgel for the management of rheumatoid arthritis. Immunological Investigations. 2024 Apr 2;53(3):490-522.
15. Das SS, Hussain MS, Tambe S, Mundhe S, Acharya A, Bhunia A, Mohanto S, Ahmed MG. Advancement on nanoparticles-based approaches for the management of rheumatoid arthritis (RA): molecular mechanism, toxicity, and clinical perspectives. Journal of Drug Targeting. 2026 May 28;34(5):721-52.
16. Kulkarni C, Sharma S, Bora PS, Verma S, Rajput S, Porwal K, Rath SK, Gayen JR, Sharma U, Chattopadhyay N. A novel extraction method enhanced the osteogenic and anti-osteoporosis effect of tea extract without any hepatotoxicity in ovariectomized rats. Frontiers in Endocrinology. 2022 Aug 8;13:951800.
17. Evans C, MacKenzie F, Marrington R. Variation in liver function testing and the effect of pyridoxal-5-phosphate on ALT, AST and FIB-4 results. Annals of Clinical Biochemistry. 2024 Nov;61(6):459-68.
18. Chavan SD, Dias RJ, Magdum CS. Allophylus cobbe Attenuates Oxidative Stress and Liver Damage in Chemically-Induced Hepatotoxicity in Wistar Rats. Tropical Journal of Natural Product Research. 2022 Mar 1;6(3).
19. Miatmoko A, Jauhari AA, Faradisa AA, Cahyani DM, Hariawan BS, Susanto J, Parumasivam T, Hendradi E, Sari R. Oral curative therapeutic study of N-nitrosodiethylamine-induced mouse liver damage of chitosan-coated ursolic acid niosomes. Scientific Reports. 2025 Jun 1;15(1):19225.
20. Tripathi PK, Gupta S, Rai S, Shrivatava A, Tripathi S, Singh S, Khopade AJ, Kesharwani P. Curcumin loaded poly (amidoamine) dendrimer-plamitic acid core-shell nanoparticles as anti-stress therapeutics. Drug development and industrial pharmacy. 2020 Mar 3;46(3):412-26.
21. Haj-Ali D, Azzam H, Aiedeh K, Alshaer W. Development of a reverse-phase HPLC method for the simultaneous determination of curcumin and dexamethasone in polymeric micelles. Future Science OA. 2025 Dec 31;11(1):2577618.

22. Sharma S, Pukale SS, Sahel DK, Agarwal DS, Dalela M, Mohanty S, Sakhuja R, Mittal A, Chitkara D. Folate-targeted cholesterol-grafted lipo-polymeric nanoparticles for chemotherapeutic agent delivery. AAPS PharmSciTech. 2020 Oct 9;21(7):280.
23. Pi C, Li L, Fu S, Yang H, Huang S, Zou Y, Zhao L, Wei Y. The Pharmacokinetics and Bio-distribution Studied by Simultaneous Analysis of Curcumin and Paclitaxel in Biosamples. Chromatographia. 2021 Oct;84(10):889-904. Khursheed R, Wadhwa S, Kumar B, Gulati M, Gupta S, Chaitanya MV, Kumar D, Jha NK, Gupta G, Prasher P, Chellappan DK. Development and validation of RP-HPLC based bioanalytical method for simultaneous estimation of curcumin and quercetin in rat's plasma. South African Journal of Botany. 2022 Sep 1;149:870-7.
24. Ponnusamy C, Krishnaswami V, Pandian S, Natesan S. In-vitro drug release and ex-vivo corneal permeation of dexamethasone and curcumin nanodispersions using facilitated simultaneous RP-HPLC technique. Analytical Chemistry Letters. 2018 May 4;8(3):311-20.
25. Ahmed OA, El-Bassossy HM, El-Sayed HM, El-Hay SS. Rp-HPLC determination of quercetin in a novel D-α-tocopherol polyethylene glycol 1000 succinate based SNEDDS formulation: Pharmacokinetics in rat plasma. Molecules. 2021 Mar 6;26(5):1435.
26. Ziaei E, Emami J, Kazemi M, Rezazadeh M. Simultaneous determination of docetaxel and celecoxib in porous microparticles and rat plasma by liquid-liquid extraction and HPLC with UV detection: in vitro and in vivo validation and application. Journal of Pharmacy and Pharmaceutical Sciences. 2020;23:289-303.
27. Ludbrook J. Statistics in biomedical laboratory and clinical science: applications, issues and pitfalls. Medical Principles and Practice. 2007 Apr 22;17(1):1-3.
28. Singh N, Choudhary R. Recent advancement in drug delivery systems for the treatment of rheumatoid arthritis. Current Drug Discovery Technologies. 2026 Mar;23(3):E15701638376838.
29. Li Y, Wei S, Sun Y, Zong S, Sui Y. Nanomedicine-based combination of dexamethasone palmitate and MCL-1 siRNA for synergistic therapeutic efficacy against rheumatoid arthritis. Drug Delivery and Translational Research. 2021 Dec;11(6):2520-9.
30. Bruno MC, Cristiano MC, Celia C, d'Avanzo N, Mancuso A, Paolino D, Wolfram J, Fresta M. Injectable drug delivery systems for osteoarthritis and rheumatoid arthritis. ACS nano. 2022 Dec 13;16(12):19665-90.
31. Hamed AM, Elbahy DA, Ahmed AR, Thabet SA, Refaei RA, Ragab I, Elmahdy SM, Osman AS, Abouelella AM. Comparison of the efficacy of curcumin and its nano formulation on dexamethasone-induced hepatic steatosis, dyslipidemia, and hyperglycemia in Wistar rats. Heliyon. 2024 Dec 30;10(24).